Oligoethylene-bridged diferrocene on Ag(110): Monolayer structures and adsorbate-induced faceting

D. Y. Zhong,[1,2] W. C. Wang,[1] R. F. Dou,[1] K. Wedeking,[3] G. Erker,[3] L. F. Chi,[1,*] and H. Fuchs[1,2]
[1]*Physikalisches Institut, Universität Münster, Wilhelm-Klemm-Strasse 10, 48149 Münster, Germany and Center for Nanotechnology (CeNTech), Universität Münster, Heisenbergstrasse 11, 48149 Münster, Germany*
[2]*Institut für Nanotechnologie, Forschungszentrum Karlsruhe, 76021 Karlsruhe, Germany*
[3]*Organisch-Chemisches Institut, Universität Münster, Corrensstrasse 40, 48149 Münster, Germany*
(Received 6 March 2007; revised manuscript received 29 June 2007; published 20 November 2007)

The self-assembly of a ferrocene (Fc) derivative, oligoethylene-bridged diferrocene (diFc), $Fc(CH_2)_{14}Fc$, on Ag(110) surface has been investigated by scanning tunneling microscopy (STM) under ultrahigh vacuum. Three ordered structures, the majority β and the minorities α and γ, are formed at monolayer coverage. In α and γ, a unit cell contains one molecule and the molecules are parallel to each other so that the distances between Fc groups and between oligoethylene chains are reduced. A unit cell contains five molecules in β: four of them are parallel to each other but not parallel to the fifth. The interaction between diFc and Ag(110), which is relatively strong in comparison to the intermolecular interaction, is dominant for the assembly of the ordered structures. The adsorption of diFc molecules induces the reorganization of substrate steps, which prefer to follow the directions of the superstructure lattice vectors, i.e., $(\mp 1,2)$ and $(\pm 3,2)$ of the Ag(110) surface. The (12 13−1) facet is formed due to step bunching at regions with high step density. By using *in situ* STM, the process of step reorganization and faceting has been observed in real time. It is concluded that the Ag adatoms play a key role on the substrate reorganization.

DOI: 10.1103/PhysRevB.76.205428 PACS number(s): 68.43.Fg, 68.37.Ef, 81.16.Dn, 81.15.Hi

I. INTRODUCTION

The interaction and interplay between adsorbed molecules and surfaces are important for understanding adsorption phenomena, catalyst, and recently epitaxial growth of functional organic materials for application in organic electronics. On one hand, due to the periodic structure of the substrate surfaces, as well as the intermolecular interactions, the molecules adsorbed on a surface tend to assemble to regular superstructures.[1] On the other hand, in some cases, the adsorbed molecules also change the structure of the surface underneath, resulting in reorganization and faceting of the substrate.[2]

Ferrocene and its derivatives are electrochemically active molecules which have been widely used as catalyst and recently have been intriguing in electrochemistry and nanoelectronics.[3–9] Novel electronic properties in nanoscale have been reported, including stochastic conductance variation,[3] reversible switching,[4] negative differential resistance,[6] etc. The adsorption and desorption of ferrocene on solid surfaces, such as Au(111),[10] Ag(100),[11–13] Cu(100),[11] and graphite,[14] have been investigated under ultrahigh vacuum (UHV). It has been found that the adsorbed ferrocene molecules are weakly bound to Ag(100) surface through the π system of the cyclopentadienyl ring and desorbed at a temperature above 250 K.[12] Although the ferrocene molecules adsorbed on Ag surface have a preferential orientation, no long-range order has been found.

Here, we report the assembly of oligoethylene-bridged diferrocene (diFc), $Fc(CH_2)_{14}Fc$ (Fc=ferrocenyl, see Ref. 15 for details about the synthesis), a ferrocene derivative consisting of two Fc groups bridged by an oligoethylene chain (Fig. 1, inset), on Ag(110) surface. By using scanning tunneling microscopy (STM), three ordered structures have been found in the monolayer (ML) film. Meanwhile, adsorbate-induced substrate reorganization has been observed without any postgrowth annealing. Using an *in situ* STM, we have investigated the substrate step reorganization in real time. The orientation of the molecules and the intermolecular and molecule-substrate interactions are discussed.

II. EXPERIMENT

The samples were prepared by means of organic molecular beam deposition (OMBD) under UHV with a base

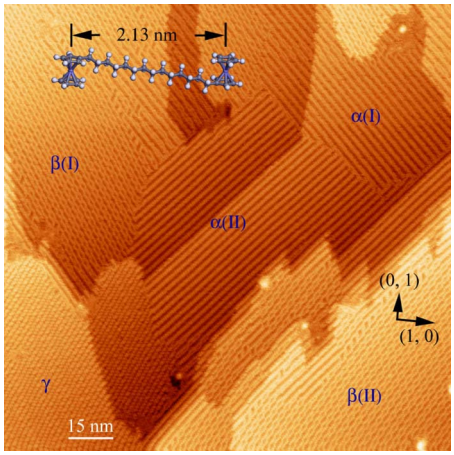

FIG. 1. (Color online) Large-scale STM image of diFc ML structures on Ag(110), 0.578 V, 0.15 nA. Three ordered structures, α, β, and γ, including two reflection domains of α [α (I) and (II)] and β [β (I) and (II)] are shown. The (1, 0) and (0, 1) directions of Ag(110) surface are notated by the arrows. Inset: Molecular structure of $Fc(CH_2)_{14}Fc$.

vacuum better than 10^{-9} mbar.[16,17] Before the deposition of organic molecules, the crystalline Ag(110) surface was sputtered by argon ions and then annealed to about 800 K repeatedly for several times. The quality of the surface was checked by low energy electron diffraction and STM. The organic source loaded in a crucible cell was degassed and purified by keeping at the sublimation temperature (413 K) for more than 1 h. The molecules were then deposited on the substrate at 310 K and the deposition time was 5 ~ 20 min for one ML (the coverage was checked by STM). After deposition, the sample was transferred from preparation chamber to STM chamber for structure analysis. Electrochemically etched tungsten tips were used for STM with constant current mode to analyze the sample at room temperature. In order to investigate the deposition process *in situ* and in real time, an OMBD instrument has been equipped on the STM chamber.[18] The STM gap voltage mentioned in the text is the sample bias with respect to the tip.

III. RESULT AND DISCUSSION

A. Monolayer structures

Three ordered ML superstructures of diFc molecules, α, β, and γ, are formed on Ag(110) surface as shown in the large-scale STM image in Fig. 1 (0.578 V, 0.15 nA). Due to the lower symmetry of the superstructures compared to the Ag(110) substrate, two reflection domains of each structure coexist in the film (the reflection domain of structure γ is not shown in Fig. 1). By estimating from a number of STM images obtained at different substrate sites, we found that structure β is the majority, which covers more than 80% of the substrate surface, while structure α and γ are much rare, which cover less than 10% and 5%, respectively.

Figures 2(a), 2(b) and 2(c) are the zoomed STM images of α, β, and γ structures, respectively. In α, all molecules are parallel to each other along the $(\pm 1,7)$ direction and rowed up along the $(\mp 1,2)$ direction of Ag(110) surface [Fig. 2(a)]. The Fc groups of the neighboring molecules tend to attract together and the oligoethylene chains are parallel to each other. Such a configuration is similar to the (−2 1 1) plane of the diFc crystal.[15] Since the Fc groups are geometrically higher than the oligoethylene chains and possess higher density of electronic states, the STM image shows parallel bright and dark stripes which correspond to the rows of the Fc groups and the oligoethylene chains, respectively. Structure β is more complicated than structure α and contains five molecules in a unit cell. Four of them are parallel to each other along the $(\pm 1,7)$ direction as those in α, while the fifth molecule is along the $(\pm 4,5)$ direction. Each Fc group has two neighbors in structure β, while it is four in structure α. Furthermore, the average area occupied by a molecule in β, 1.79 nm^2, is greater than that of α, 1.54 nm^2. The information about the molecular orientation was obtained from the step edges and the defects on the terraces. The inset of Fig. 2(b) shows a region (7×7 nm^2) at the boundary between α and β domains. Six molecules (two of them denoted by the short lines) are arranged shoulder by shoulder following the orientation of the fifth molecule in β structure. The γ structure is well similar to the α structure, with all molecules parallel to each other and oriented along the $(\pm 1,7)$ direction. However, the molecules are rowed up along the $(\mp 1,3)$ direction of Ag(110), rather than along $(\mp 1,2)$. The average area occupied by a molecule in structure γ is 2.01 nm^2, much larger than those of α and β. As shown in Fig. 2(c), there are some bright spots marked by circles on a line. Each spot contains four small bright spots, corresponding to four Fc groups together. These defects are due to the offset of molecules along (0, 1) direction of Ag(110), from $(\mp 1,3)$ site to $(\mp 1,2)$ site, so that the four molecules adopt the configuration like structure α.

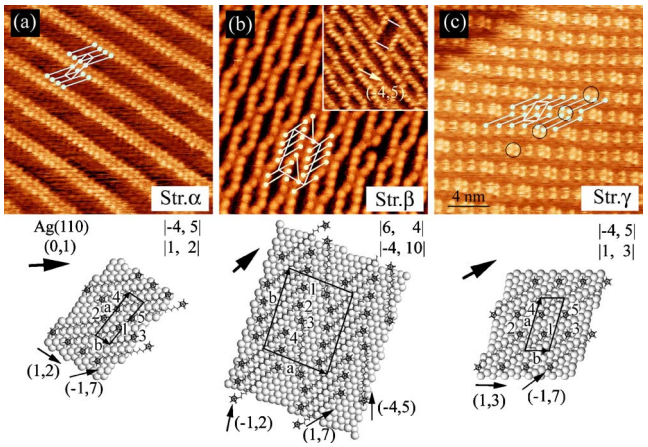

FIG. 2. (Color online) STM images (top) and proposed structural models (bottom) of diFc monolayers on Ag(110). In the models, the relative position of the molecules to the substrate and the orientation of the Fc groups are arbitrarily chosen. The scale bar in (c) is also applicable for (a) and (b). (a) α, 0.16 V, 0.2 nA. (b) β, −2.1 V, 0.15 nA. Inset: A region (7×7 nm^2) at the boundary between α and β domains with six molecules (two of them denoted by short lines) arranged shoulder by shoulder, following the orientation of the fifth molecule in β structure, 0.25 V, 0.15 nA. (c) γ, 0.15 V, 0.15 nA.

It has been reported that a single ferrocene molecule adsorbed on Ag(100) and graphite surfaces is oriented with the molecular axis perpendicular to the surfaces, while it is oriented with the axis parallel to the surface when adsorbed on the Cu(100) surface.[11] In the case of diFc molecules, the configurations of the two Fc groups in a molecule are correlated and therefore the situation may be different from that of a single ferrocene. Unfortunately, due to the thermal vibration of the molecules at the equilibrium site, it is difficult to obtain the detailed information about the orientation of the Fc groups by STM at room temperature. We proposed in our models that the Fc groups adsorbed on the Ag(110) surface with their axis perpendicular to the surface, similar to the single Fc molecules adsorbed on Ag(100) surface reported in Refs. 11 and 13.

The proposed models of structures α, β, and γ are presented below the STM images in Fig. 2(a) (the relative positions of the molecules to the substrate are arbitrarily chosen). In Table I, the geometrical data of the proposed models are listed, including the relationship matrix with the substrate, the base vectors, the orientation of molecules, the dis-

TABLE I. Geometrical parameters of the proposed models and the (−2 1 1) plane from the molecular crystal. In the table, the relationship matrix with the substrate, the base vectors, the orientation of molecules, the distance between the neighboring Fc's (iron-iron distance), the distance between the parallel oligoethylene chains, and the occupied area per molecule are listed. The former values of the lattice parameters (a, b, and θ) are from the models and the latter from the experiments. In the field of Fc-Fc distance, the Fc groups are identified by the subscripts, which correspond to the notations in Fig. 2. The notations for the (−2 1 1) plane is similar to those for the structures α and γ.

Structure	α	β	γ	(−2 1 1)
Matrix	$\begin{vmatrix}\pm 4 & 5\\ \mp 1 & 2\end{vmatrix}$	$\begin{vmatrix}\pm 6 & 4\\ \mp 4 & 10\end{vmatrix}$	$\begin{vmatrix}\pm 4 & 5\\ \mp 1 & 3\end{vmatrix}$	
a (nm)	2.18/2.2	2.71/2.7	2.18/1.9	2.06
b (nm)	0.71/0.7	3.32/3.3	0.96/1.0	1.36
θ (°)	83.8/85	94.3/95	73.8/68	79.5
Mole.	1	5	1	2
Orientation	(±1,7)	(±1,7) (±4,5)	(±1,7)	
Fc-Fc (nm)	d_{12}=0.71 d_{13}=0.71 d_{14}=0.62 d_{15}=0.73	d_{12}=0.71 d_{23}=0.63 d_{34}=0.79	d_{12}=0.96 d_{13}=0.96 d_{14}=0.77 d_{15}=1.16	d_{12}=0.64 d_{13}=0.72 d_{14}=0.65 d_{15}=0.58
Chain-chain (nm)	0.50	0.50	0.54	0.44
Area/mole. (nm)	1.54	1.79	2.01	1.38

tance between neighboring Fc groups, the distance between the parallel oligoethylene chains, and the occupied area per molecule. The relationship matrices are predicted directly based on the length and angle data from the STM measurements. The difference of the experimental values from the models is typically less than 5%. For example, the lengths of the base vectors and the angle enclosed by the base vectors of structure β obtained from experiments are a=2.7 nm, b =3.3 nm, and θ=95°, respectively, which are quite close to the values from the proposed model listed in Table I. The relative positions and orientations of the molecules in the unit cells are chosen so that the overlap between the molecules is minimized. For sake of comparison, the data of the (−2 1 1) plane of the crystalline structure are listed together (see Ref. 15). In the (−2 1 1) plane, all the molecules lie in the same plane and are parallel to each other [similar to Fig. 2(a)]. A half number of the molecules are with the axis of the Fc group perpendicular to the plane, while the other half number of the molecules parallel. These two kinds of molecules interlace so that the distances between the oligoethylene chains are efficiently reduced and each Fc neighbors with four Fc groups. Three of the neighbors are arranged face to edge as in Fc crystal.[19–21] As a result, the molecules in (−2 1 1) plane are highly packed and each occupies an area of 1.38 nm^2. Due to the molecule-substrate interaction, the assembly of organic molecules on a substrate usually does not adopt a highly packed structure. The distance between the neighboring Fc groups and between neighboring parallel oligoethylene chains in ML superstructures are larger than those in the bulk. All of the three ordered structures we obtained have an area per molecule value larger than that of the (−2 1 1) plane. According to the data shown in Table I it is believed that the van der Waals interaction between the molecules in the ML film are weakened to some extent and the molecule-substrate interaction is dominant for the formation of the ML structures.

According to the models, one can compare the intermolecular interaction in the three structures with each other. The orientation of the fifth molecule in structure β is disadvantageous for intermolecular interaction. On one hand, the oligoethylene chain of the fifth molecule has no neighboring chains. On the other hand, there are only two neighboring Fc groups for each Fc group in structure β. As a result, the intermolecular interaction in β is weakened in comparison to α. When comparing γ with α structure, we found that both the distances between Fc's and between oligoethylene chains in γ are greater than those in α, implying that the intermolecular interaction in γ is weaker than in α. Furthermore, the area occupied per molecule in α structure is the smallest among the three structures. Thus, we conclude that the intermolecular interaction in α is relatively stronger than both in β and γ. However, according to our experiments, the β structure is the majority at room temperature. The most energetically favorable configuration in β is probably due to the enhancement of the substrate-molecule interaction.

B. Step edge reorganization

Besides the ordered ML structures formed on the terraces of Ag(110) surface, we have found that the substrate steps are reorganized due to the adsorption of diFc molecules. As shown in Fig. 3(a), there are two types of reorganization, single-step reorganization and step bunching. The single-step reorganization exists at regions of the substrate with low density of steps and wide terraces (>50 nm), while the step bunching and faceting exist at regions with high density of steps and narrow terraces (<10 nm).

Figure 3(b) is the zoomed STM image at region denoted by rectangle b in Fig. 3(a), showing the detailed information of the single-step reorganization. Both the upward and downward terraces near the step are covered with molecules in β structure. The step is along the direction of the shorter base vector of β, i.e., the (3, 2) direction of Ag(110) surface. Furthermore, there are kinks on the step with a width about 3.5 nm, consistent with the length of the longer base vector of β [marked by the arrow in Fig. 3(b)]. In Fig. 3(d), a model is proposed to describe the single-step reorganization at area denoted by rectangle d in Fig. 3(b).

Figure 3(c) is the zoomed STM image of region denoted by rectangle c in Fig. 3(a), showing the step bunching and faceting induced by the adsorption of diFc molecules. The sawtoothlike morphology contains two edges: One is straight and regular along the shorter base vector of α structure, i.e., (−1,2) direction of the Ag(110) surface, and the other is irregular on the whole along (1, 2) direction of structure α, i.e., (2, 9) direction of the Ag(110) surface. The plane angle between the Ag(110) and the facet at the straight edge is about 4°. The width between the bunched steps is 2.2 nm, as

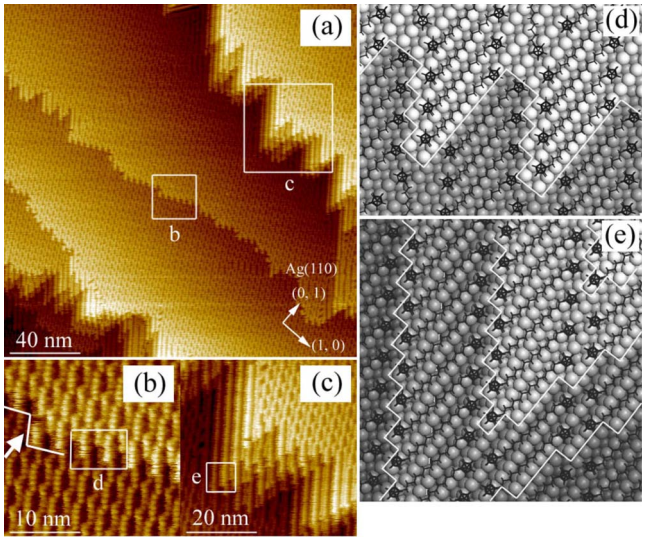

FIG. 3. (Color online) Substrate step reorganization induced by adsorption of diFc molecules. (a) Large-scale STM image (−1.5 V, 0.2 nA), showing two typical types of step reorganization, single-step reorganization and step bunching. (b) Zoomed STM image [rectangle b in (a)] showing the single-step reorganization, −1.5 V, 0.2 nA. The arrow denotes a kink of the reorganized step edge. (c) Zoomed STM image [rectangle c in (a)] showing the step bunching, −1.5 V, 0.2 nA. (d) Proposed model for single-step reorganization. (e) Proposed model for step bunching.

measured from the STM image. The facet belongs to the (12 13 −1) plane of Ag face-centered cubic (fcc) lattice, which is 3.96° tilted with respect to the (110) plane and contains a series of parallel steps along (−1,2) of (110) surface and narrow terraces (2.1 nm wide). A model is proposed in Fig. 3(e), which corresponds to the region denoted by rectangle e in Fig. 3(c). The results described above indicate that the steps prefer to be reorganized along the shorter base vectors of the upward superstructures, consistent with the former studies.[2]

In general, the low-index planes are more energetically stable than high-index facets due to the lower surface energy. The adsorbate-induced faceting originates from the adsorbate-substrate and intermolecular interactions, which change the surface energy and the thermodynamic balance on the surface. The molecules adsorbed on a flat terrace interact with the substrate in one direction, while at a step edge they interact with the substrate at two directions. The molecule-substrate interaction is strengthened at step edges, which makes the adsorption more stable. Some organic molecules that contain electronegative elements, such as O and N atoms in their functional groups, have been reported to induce facets when adsorbed on Cu(110) and Ag(110) surfaces.[2,23–25] Generally, these molecules contain carboxylate group and are chemisorbed on the surfaces. Due to the poor diffusion ability, the faceting is obtained at elevated temperatures, for example, annealing to 540 K for *p*-aminobenzoic acid on Cu(110),[22] 375 K for (S)-glutamic acid,[24] and 430 K for 4-[trans-2-(pyrid-4-yl-vinyl)] benzoic acid on Ag(110).[25] In case of diFc on Ag(110), annealing is not necessary for the facet formation. Since the diFc molecule does not contain carboxylate or other active groups which aid to form chemical bond with the substrate, we believe that the faceting process originates from other kind of molecule-substrate interactions such as charge transfer. Both the ordered ML structures and the adsorbate-induced step reorganization imply that a relative strong interaction exists between the diFc molecules and the Ag(110) surface.

C. Real-time scanning tunneling microscopy observation of step reorganization and faceting

Although the step reorganization and faceting induced by adsorbates in a number of adsorbate-substrate systems, including metal on metal, small molecules on metal, and organic molecules on metal,[2] have been obtained, no real-time observation has been obtained. It is known that the long-range mass transport of the substrate is essential for the step reorganization and faceting induced by adsorbates. However, it is an open question what is the diffusing species for the step reorganization, the bare substrate atoms, or the substrate atoms bonded to the adsorbates. Here, we use *in situ* STM to investigate the evolution of the steps during the deposition of organic molecules.[18]

Figure 4(a) shows the STM image of the Ag(110) substrate before deposition. At the step edges or on the terraces, there are small vacancies with one-layer (short black arrow) or three-layer (short white arrow) depth, as well as small islands with two to three layer height. A screw defect exists at the step edge 2. At room temperature, the Ag adatoms are diffusing on terraces as two-dimensional gas, under a balance between the attachment of adatoms to the step edge and the detachment of the atoms from the step edge.[26] As a result, the STM images of the step edge of Ag(110) surface are not sharp, as shown in inset of Fig. 4(a).

Figures 4(b)–4(e) show the selected real-time STM images obtained during a ML deposition process. The total deposition time is 18 min and the STM scanning speed is 2 min/image (containing nine images, −1.0 V, 0.2 nA). At submonolayer regime [(b), (c), and (d)], only domains with localized orderliness are found on the surface. Furthermore, the structures are not stable and stochastic transitions between ordering and disordering and between different superstructures have been observed. At regime near a full ML [Fig. 4(e)], stable β structure with large domains is formed. The structure is not perfect with defects probably due to the scanning of the STM tip. During the deposition, the step edges migrate and the terraces grow at some positions and time, while decay at some other positions and time. In general, the terraces tend to grow along the (0, 1) direction. An obvious example is step 6, which grew along the (0, 1) and was bunched with step 7 at last. It is interesting that the small islands on the substrate have no pinning effect on the evolution of the step edges. Most vacancies on the substrate are filled during the deposition. Two of them [arrowed in Fig. 4(a)], however, induce grooves on the surface.

The final reorganized structures of the step edges induced by the deposition of organic molecules are presented in Fig. 4(f), which were obtained at the region near the upper left corner of Figs. 4(a)–4(e). At some areas near step 9, the steps

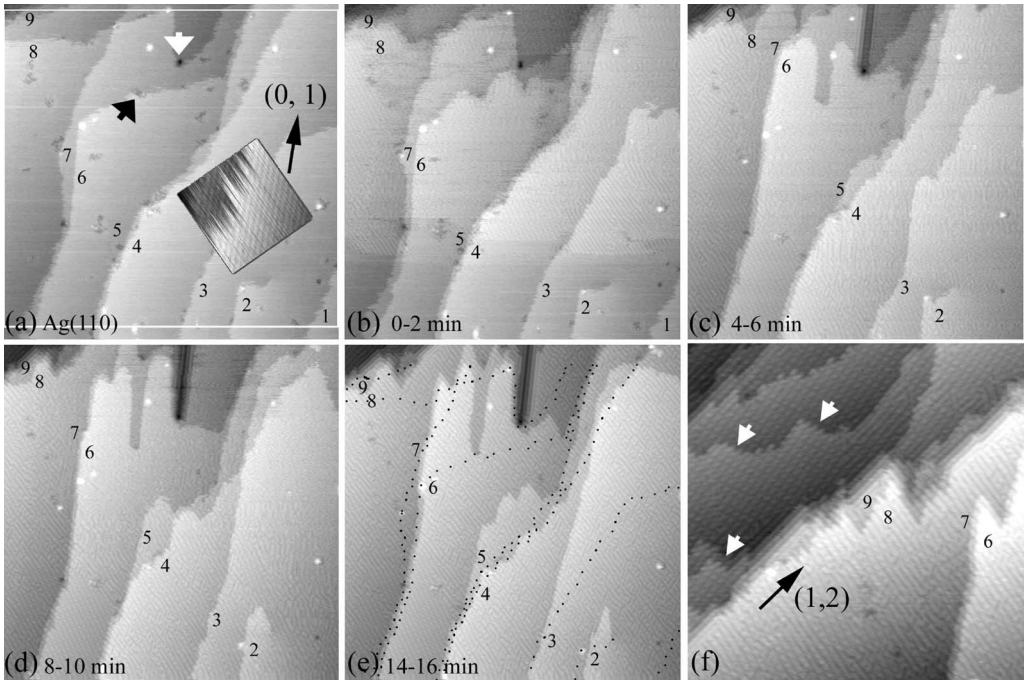

FIG. 4. *In situ* STM observation of the step evolution ([(a)–(e)] −1.0 V, 0.2 nA, 200×200 nm^2; (f) −1.0 V, 0.2 nA, 120×120 nm^2). (a) Ag(110) substrate before deposition. Short arrows: Vacancies. Inset: Zoomed image of Ag(110) surface, 0.7 V, 0.3 nA, 10×10 nm^2. [(b)–(e)] STM sequence showing a ML deposition process. Scanning speed, 2 min/frame; total time, 18 min. (f) STM image at the region near the upper left corner of (a)–(e), showing the final step reorganization and faceting.

were bunched together along the (1, 2) direction, which was observed in real time as shown in Figs. 4(a)–4(e). In addition, the bunching of steps 6 and 7 caused by the growth of terrace 6 during the deposition process exhibits tendency aligned along the (−1,2) direction. The arrowed step edges, which are out of the scanning region in Figs. 4(a)–4(e), exhibit the single-step reorganization as described in Sec. III B.

In Fig. 5, the area proportions of the terrace growth and decay to the total scanning area [denoted by the rectangle in Fig. 4(a)] are counted based on the STM sequence shown in Fig. 4. The filled and unfilled bars denote the terrace growth and decay, respectively. Before deposition, the growth and

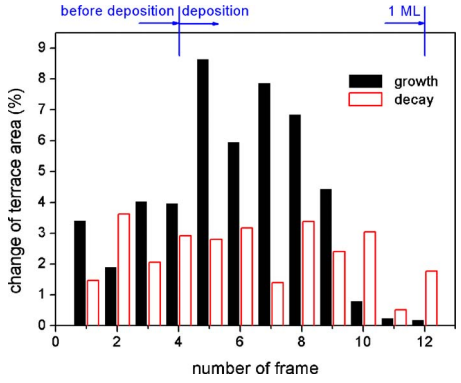

FIG. 5. (Color online) Statistics of the proportion of growth (filled bars) and decay areas (hollow bars) of the substrate terraces during the deposition process. The deposition process started at frame 4 and a coverage about 1 ML was obtained at frame 12.

decay areas of the terraces have a proportion about 3%. At the submonolayer regime, the proportion of the growth is increased to about 8% and decreased to less than 1% at regime near ML coverage, while the proportion of the decay has no obvious increase at submonolayer regime and is decreased to about 1% at regime near ML coverage. The relatively large proportion of growth at the submonolayer regime is from both the attachment of the Ag adatoms on terraces and the decay of the atoms from step edges. The proportion of decay is contributed from two situations: One is the erosion of the terraces which exist before the deposition of the organic molecules; the other is the ditching process and the groove formation.

The net growth of terraces in total during the deposition estimated from Fig. 5 is about 20%, or 0.2 ML, which is much higher than the equilibrium Ag adatom density at room temperature.[26] This suggests that not only the adatoms in the scanning region but also the adatom outside the scanning region contribute to the terrace growth shown in Fig. 4. In other words, the net growth of terraces may be greater at some regions than other regions and the average proportion of the net growth may be much less than 20%, given an equilibrium Ag adatom density of 0.05 ML.[26] We explain that the fluctuation of the net growth may originate from the thermodynamic fluctuation and/or the nonuniformity of the step density on the substrate.

It should be emphasized that the faceting takes place during the molecular adsorption on the surface near room temperature and no annealing process was used. Each adsorbed diFc molecule, which lies on the surface with its carbon chain parallel to the surface, is interacting with more than

one Ag atom from the surface. Although both the molecules and the Ag adatoms are able to easily migrate thermally activated at room temperature, it is more difficult to activate a cluster containing a diFc bound with a few Ag atoms. We believe that it is the bare substrate atoms, not the substrate atoms bonded to the adsorbates, that correspond to the long-range mass transport for the step reorganization and faceting. At submonolayer regime, the adsorbed organic molecules and the Ag adatoms coexist on the terraces. The Ag adatoms diffuse on the surface and bond at the step edges of the surface. On the other hand, the atoms at the step edges will be detached onto the terraces as adatoms. When increasing the coverage of the molecules, the total number of Ag adatoms will be decreased. Since it is relatively easier to diffuse along the (0, 1) direction than along the (1, 0) direction, there is greater probability for the adatoms to attach on the steps along the (1, 0) direction than along the (0, 1) direction, resulting in the preferential growth of terraces along the (0, 1) direction. The attachment of adatoms on the step edges results in the fact that the proportion of the terrace growth is greater than that of decay at submonolayer regime, as shown in Fig. 5. At coverage near ML, most of the Ag adatoms are attached on the step edges and the growth rate of the terraces decreased.

IV. CONCLUSION

Ordered ML structures of oligoethylene-bridged diFc molecules are assembled on Ag(110) surface. The molecules are oriented mainly along the (1, 7) direction of the Ag(110). The interaction between diFc and Ag(110), which is relatively strong in comparison to the intermolecular interaction, is dominant for the assembly of the ordered structures. The substrate surface is reorganized and the $(12\ 13\ -1)$ facet is formed due to the adsorption of diFc molecules. By using an *in situ* STM, the substrate reorganization has been observed in real time during the deposition of molecules. It has been found that the terraces grow along the (0, 1) direction of Ag(110), surface, and the Ag adatoms make a key role on the reorganization.

ACKNOWLEDGMENTS

This work was supported by the Sonderforschungsbereich (SFB) 424 of Deutsche Forschungsgemeinschaft (DFG). D.Y.Z. thanks the financial support from Helmholtz Gemeinschaft.

*Corresponding author; chi@uni-muenster.de

[1] D. E. Hooks, T. Fritz, and M. D. Ward, Adv. Mater. (Weinheim, Ger.) **13**, 227 (2001).
[2] Q. Chen and N. V. Richardson, Prog. Surf. Sci. **73**, 59 (2003).
[3] R. A. Wassel, R. R. Fuierer, N. Kim, and C. B. Gorman, Nano Lett. **3**, 1617 (2003).
[4] C. Engtrakul and L. R. Sita, Nano Lett. **1**, 541 (2001).
[5] P. Kruse, E. R. Johnson, G. A. DiLabio, and R. A. Wolkow, Nano Lett. **2**, 807 (2002).
[6] C. B. Gorman, R. L. Carroll, and R. R. Fuierer, Langmuir **17**, 6923 (2001).
[7] Q. Li, G. Mathur, S. Gowda, S. Surthi, Q. Zhao, L. Yu, J. S. Lindsey, D. F. Bocian, and V. Misra, Adv. Mater. (Weinheim, Ger.) **16**, 133 (2004).
[8] A. V. Tivanski and G. C. Walker, J. Am. Chem. Soc. **127**, 7647 (2005).
[9] H. D. Sikes, J. F. Smalley, S. P. Dudek, A. R. Cook, M. D. Newton, C. E. D. Chidsey, and S. W. Feldberg, Science **291**, 1519 (2001).
[10] K.-F. Braun, V. Iancu, N. Pertaya, K.-H. Rieder, and S.-W. Hla, Phys. Rev. Lett. **96**, 246102 (2006).
[11] C. Waldfried, D. Welipitiya, C. W. Hutchings, H. S. V. de Silva, G. A. Gallup, P. A. Dowben, W. W. Pai, J. Zhang, J. F. Wendelken, and N. M. Boag, J. Phys. Chem. B **101**, 9782 (1997).
[12] D. Welipitiya, P. A. Dowben, J. Zhang, W. W. Pai, and J. F. Wendelken, Surf. Sci. **367**, 20 (1996).
[13] C. M. Woodbridge, D. L. Pugmire, R. C. Johnson, N. M. Boag, and M. A. Langell, J. Phys. Chem. B **104**, 3085 (2000).
[14] P. J. Durston and R. E. Palmer, Surf. Sci. **400**, 277 (1998).
[15] K. Wedeking, Z. Mu, G. Kehr, J. C. Sierra, C. M. Lichtenfeld, S. Grimme, G. Erker, R. Fröhlich, L. Chi, W. Wang, D. Zhong, and H. Fuchs, Chem.-Eur. J. **12**, 1618 (2006).
[16] D. Y. Zhong, F. Lin, L. F. Chi, Y. Wang, and H. Fuchs, Phys. Rev. B **71**, 125336 (2005).
[17] F. Lin, D. Y. Zhong, L. F. Chi, K. Ye, Y. Wang, and H. Fuchs, Phys. Rev. B **73**, 235420 (2006).
[18] R. Nowakowski, C. Seidel, and H. Fuchs, Surf. Sci. **562**, 53 (2004).
[19] D. Braga and F. Grepioni, Organometallics **11**, 711 (1992).
[20] J. D. Dunitz, L. E. Orgel, and A. Rich, Acta Crystallogr. **9**, 373 (1956).
[21] F. Maharaj, A. Mcdonagh, M. Scudder, D. Craig, and I. Dance, CrystEngComm **5**, 305 (2003).
[22] Q. Chen, D. J. Frankel, and N. V. Richardson, Langmuir **17**, 8276 (2001).
[23] F. M. Leibsle, S. Haq, B. G. Frederick, M. Bowker, and N. V. Richardson, Surf. Sci. Lett. **343**, L1175 (1995).
[24] T. E. Jones and C. J. Baddeley, Langmuir **21**, 9468 (2005).
[25] J. I. Pascual, J. V. Barth, G. Ceballos, G. Trimarchi, A. De Vita, K. Kern, and H.-P. Rust, J. Chem. Phys. **120**, 11367 (2004).
[26] W. W. Pai and J. E. Reutt-Robey, Phys. Rev. B **53**, 15997 (1996).